FAILURE BEHAVIOUR OF TRIAXIAL BRAIDED COMPOSITES

Tobias Wehrkamp-Richter[1], Silvestre T. Pinho[2], Roland Hinterhölzl[3]

[1]Institute for Carbon Composites, Technische Universität München, Faculty for Mechanical Engineering, Boltzmannstr. 15, D-85748 Garching b. München, Germany
Email: wehrkamp-richter@lcc.mw.tum.de, Web Page: http://www.lcc.mw.tum.de/en

[2]Department of Aeronautics, Imperial College London, SW7 2AZ London, United Kingdom
Email: silvestre.pinho@imperial.ac.uk, Web Page: http://www.imperial.ac.uk/people/silvestre.pinho

[3]Institute for Carbon Composites, Technische Universität München, Faculty for Mechanical Engineering, Boltzmannstr. 15, D-85748 Garching b. München, Germany
Email: hinterhoelzl@lcc.mw.tum.de, Web Page: http://www.lcc.mw.tum.de/en

Keywords: Braided Composites, Failure, Damage, Unit Cell Modelling,

Abstract
In the presented work, we propose a framework for predicting the non-linear mechanical response of triaxial braided composites using meso-scale finite element unit cells. Based on a reduced unit cell concept which exploits symmetries to minimise computational expense, a compacted and interpenetration-free yarn geometry is created within a three stage simulation process. Out-of-plane periodic boundary conditions allow an implicit consideration of the compaction of multiple braid plies in different nesting configurations, which further enables us to render high global fibre volume fractions (55-60%) using experimentally determined intra-yarn fibre volume fractions. Numerical predictions are compared to experimental data in terms of stress-strain curves.

1. Introduction

Applying new lightweight materials, such as carbon fibre reinforced plastics (CFRP) in the automotive industry allows a significant reduction in structural weight and carbon dioxide emissions. In these high-volume production industries, current manufacturing technologies face a twofold challenge: cost and cycle time. Braiding combines an automated and reproducible process together with an excellent rate of material deposition for mass-production of high performance structures. Yarns of several thousand carbon fibres are intertwined and positioned on a mandrel to produce geometries with complex cross-sections. Accurately modelling the mechanical response of 2D braided composites, however, remains a challenging task due to their textile nature, which includes out-of-plane waviness, interactions between intertwining yarns and nesting of multiple plies in the through-thickness direction.

Numerical modelling using meso-scale finite-element (FE) unit cell models provides a powerful tool to study the material behaviour of braided composites. Typically, a representative domain of the internal textile geometry is considered, wherein the constituent reinforcing yarns are explicitly modelled as solid continua. In the presented work, we propose a modelling framework for predicting the

Excerpt from ISBN 978-3-00-053387-7

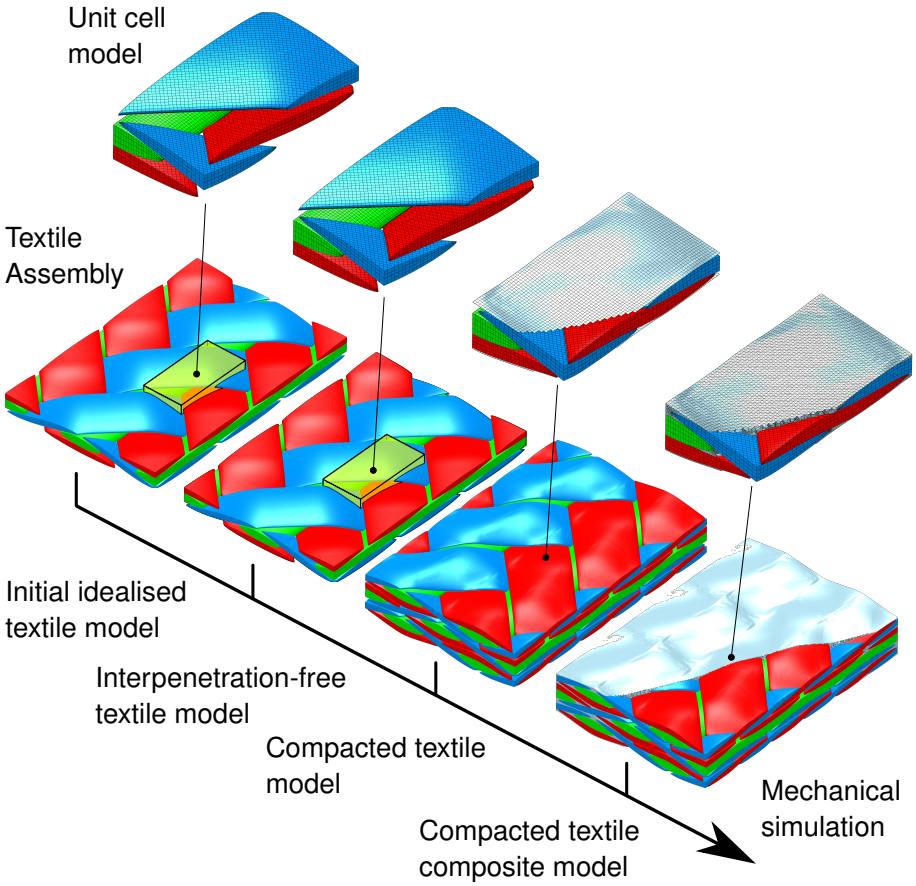

Figure 1: Roadmap and data flow for generating a realistic unit cell model

mechanical response of triaxial braided composites using FE unit cells with realistic geometry.

2. Modelling Framework

2.1. Roadmap and Dataflow

The modelling procedure is schematically shown in Fig. 1. Based on a reduced unit cell concept to minimise computational expense developed by De Carvalho et al. [1], a compacted and interpenetration-free yarn geometry is created within a three stage simulation process. In the first step, a nominal geometry is constructed from user-defined input parameters, such as braiding angle, yarn spacing and its respective cross-sectional shape. As a result of the absence of initial contact between intertwining yarns at this stage, local volumetric interpenetrations present in the model are resolved in a subsequent fictitious thermal step, in which contact is established within the entire unit cell. In the final step, the unit cell is compacted to the desired FVF using flexible membranes. Special out-of-plane periodic boundary conditions allow an implicit consideration of the compaction of multiple braid plies in different nesting configurations, which further enables us to render global FVFs of $55 - 60\%$ without assuming an unrealistically high FVF inside the yarns. Finally, the deformed hexahedral yarn mesh is used in a series of boolean operations to create an inconsistent tetrahedral matrix mesh, and both meshes are coupled using a cohesive contact formulation in order to investigate the mechanical behaviour of the braided composite.

Excerpt from ISBN 978-3-00-053387-7

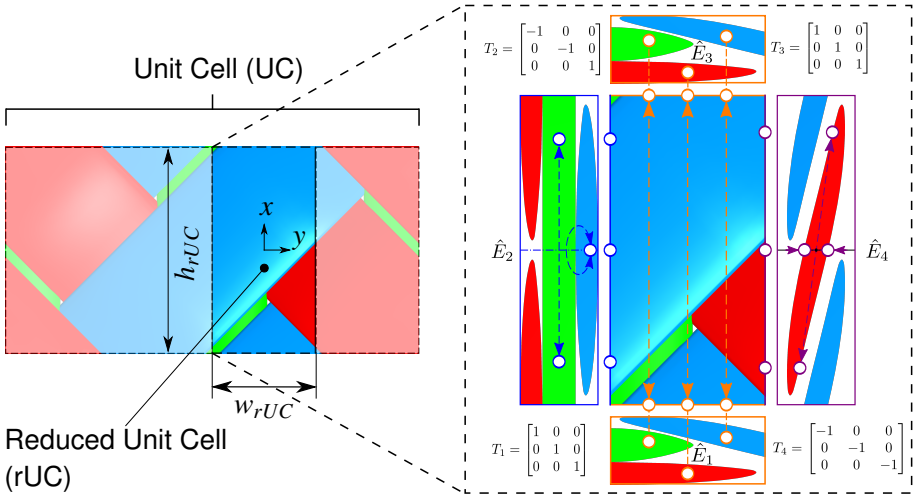

Figure 2: Reduced unit cell with periodic boundary conditions

2.2. Periodic Boundary Conditions

In order to minimise computational effort, a reduced unit cell (rUC) for triaxial braided composites is derived on the basis of the equivalence framework for periodic structures developed by De Carvalho et al. [1]. In general, the periodic displacement boundary conditions for a deformable periodic body which includes symmetries can be written as

$$u(A) - \gamma \cdot T \cdot u(\hat{A}) = -\langle \varepsilon \rangle \cdot T \cdot x^{O_{\hat{E}}} \tag{1}$$

where u denote the displacements of equivalent points at a periodic boundary expressed by their coordinate vectors A and $\hat{A}$, respectively. T is a transformation matrix between adjacent sub-domains, $\langle \varepsilon \rangle$ is the volume averaged strain tensor and $\gamma = \pm 1$ describes the load reversal factor. Considering the rUC shown in Fig. 2, the PBCs can be implemented by enforcing a series of linear constraint equations between displacements of equivalent nodes on the periodic boundary mesh.

3. Constitutive Model

The non-linear mechanical response of each yarn is modelled using a constitutive law proposed by Pinho [2]. As one of the best performing failure theories benchmarked in the World Wide Failure Exercise (WWFE) [3], this physically-based smeared crack model considers currently known failure processes in composites under three-dimensional stress states, such as matrix cracking, matrix plasticity, fibre kinking and fibre tensile failure. Whereas the latter is predicted using a maximum stress criterion, the coincident fibre kinking and splitting failure indices are evaluated on a rotated fracture plane aligned with the formation of a possible kink band by:

$$FI_{KINK} = FI_{SPLIT} = \left(\frac{\tau_{23}^{m}}{S_{T}^{is} - \eta_{T} \cdot \sigma_{2}^{m}} \right)^{2} + \left(\frac{\tau_{12}^{m}}{S_{L}^{is} - \eta_{L} \cdot \sigma_{2}^{m}} \right)^{2} + \left(\frac{\langle \sigma_{2}^{m} \rangle}{Y_{T}^{is}} \right)^{2} \tag{2}$$

where S_{L}^{is} and S_{T}^{is} are the in-situ longitudinal and transverse shear strengths, Y_{T}^{is} is the in-situ transverse tensile strength and η_L and η_T are friction coefficients on the corresponding fracture plane.

Excerpt from ISBN 978-3-00-053387-7

These two failure modes are then distinguished based on the magnitude of acting longitudinal compressive stress, which is important for further failure propagation.

Matrix cracking is predicted using a modified version of the Mohr-Coulomb failure criterion with a quadratic stress interaction on a rotated fracture plane given by

$$FI_M = \left(\frac{\tau_T^m}{S_T^{is} - \eta_T \cdot \sigma_N^m} \right)^2 + \left(\frac{\tau_L^m}{S_L^{is} - \eta_L \cdot \sigma_N^m} \right)^2 + \left(\frac{\langle \sigma_N^m \rangle}{Y_T^{is}} \right)^2 \tag{3}$$

where σ_N, τ_L and τ_T are the components of the traction vector acting on a possible fracture plane obtained by stress transformation. The normal traction component σ_N only contributes to failure onset for positive values attributed to crack opening, whereas a negative or compressive value inhibits failure onset through frictional mechanisms.

Non-linearities before failure onset due to matrix induced plasticity are considered through a decomposition of the total strain tensor into an elastic and plastic part, which yields a constitutive law in the form of

$$\sigma = E^0 : (\varepsilon - \varepsilon_{pl}) \tag{4}$$

where E^0 denotes the elasticity tensor of the undamaged material, σ is the effective stress tensor and ε and ε_{pl} are the total and plastic strain tensors. The latter irreversible part can be obtained from a degradation of the secant shear and transverse moduli represented by arbitrary user-defined analytical functions in the form of

$$G_{12}^{nl} = G_{13}^{nl} = f_1(\varepsilon_{eq}) \qquad E_2^{nl} = E_3^{nl} = f_2(\varepsilon_{eq}) \tag{5}$$

in which the irreversible equivalent strain is further defined as

$$\varepsilon_{eq} = \sqrt{(\varepsilon_2 - \varepsilon_3)^2 + \gamma_{12}^2 + \gamma_{13}^2 + \gamma_{23}^2}. \tag{6}$$

The degradation functions defined by equation 5 are determined experimentally under the respective uniaxial loading conditions. After failure onset, the traction components on the fracture plane are degraded using a bilinear energy based softening law for fibre tensile failure and kinking, and a trilinear law for matrix cracking.

4. Results and Discussion

In the presented paper, the previously established framework is applied to predict the non-linear mechanical response for a $[0/\pm 30]$ and a $[0/\pm 45]$ triaxial braid manufactured from Toho-Tenax HTS40 F13 12K yarns for both the axial and braid yarns in combination with a Hexcel Hexflow RTM6 epoxy resin. Geometry data was obtained from measurements on undamaged CT data and polished micro-sections and is summarised in Table 1. Numerical results are compared to experiments in terms of stress-strain curves for loading in the take-up direction, parallel to the axial yarns, and in

Excerpt from ISBN 978-3-00-053387-7

transverse direction. For the numerical predictions, two out-of-plane nesting cases are considered. Firstly, a regular stacked configuration, in which nesting occurs such that the top and bottom layers are inverted to allow axial yarns to nest into gaps forming between braid yarns. Secondly, an axial shift is added to the top and bottom layer.

Table 1: Geometry data

θ (°)	$\varphi_{F,rUC}$ (-)	κ_a (-)	κ_b (-)	$\bar{t}_{rUC,c}$ (um)	s_a (um)	w_a (um)	t_a (um)	s_b (um)	w_b (um)	t_b (um)
30	0.56	0.66	0.70	764	3354	2122	452	2905	2695	326
45	0.55	0.66	0.70	776	4232	2340	440	2992	2716	327

4.1. Loading in axial direction

The stress-strain curves for loading in axial direction (11) are displayed in Fig. 3 for the $[0/\pm 30]$ and $[0/\pm 45]$ braid, respectively. As the load direction is aligned with the axial yarn, a rather linear behaviour up to final failure caused by rupture of the axial yarns can be observed in the experiments coinciding with the numerical predictions. The shifted configuration generally yields a lower failure stress compared to the regular stack configuration, which can be attributed to its higher degree of yarn distortion after compaction. The resulting geometry not only yields more severe stress concentrations inside the yarns, but can also trigger preliminary delamination of the slightly undulated axial yarns which then subsequently induces secondary fibre failure. Considering scatter in the experiments, the upper and lower bounds in ultimate strength are well predicted by the two nesting configurations.

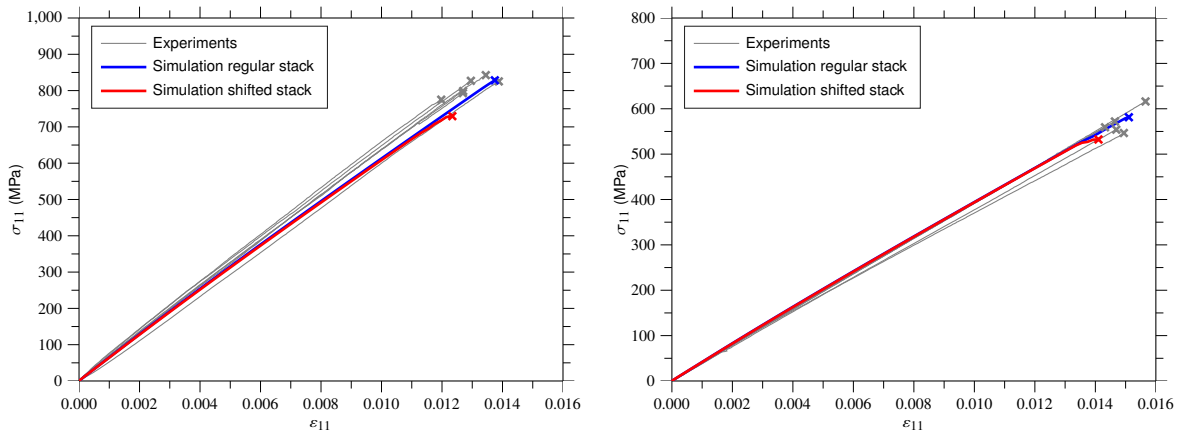

Figure 3: Stress-strain curves for loading in axial (11) direction (a) $[0/\pm 30]$ (b) $[0/\pm 45]$

4.2. Loading in transverse direction

Severe non-linearities exist in all braid architectures for loading in the transverse (22) direction. The $[0/\pm 30]$ braid features a complex damage behaviour, which is shown in Fig. 4 (a). Here, the material response can be separated into three distinct domains up to final failure: the elastic domain, the damage progression domain and the saturation domain. This behaviour is predicted accurately by the regularly stacked unit cell model. When a critical load level is reached in the linear domain, matrix cracks form in the axial yarns and initiate further cracking inside the braid yarns. As the strain further

Excerpt from ISBN 978-3-00-053387-7

increases, the load level exhibits a stable plateau as a result of progressive damage development. When a critical crack density is reached, a small increase in load can be observed before final failure. The $[0/\pm 45]$ braid exhibits a similar material behaviour, with the first cracks appearing again in the axial yarns subjected to transverse tension. However, the braid yarns contribute significantly more stiffness to the transverse direction, only a gradual degradation is observed. While the initiation point for this degradation is captured well, the severity of the overall degradation due to matrix cracking is underestimated.

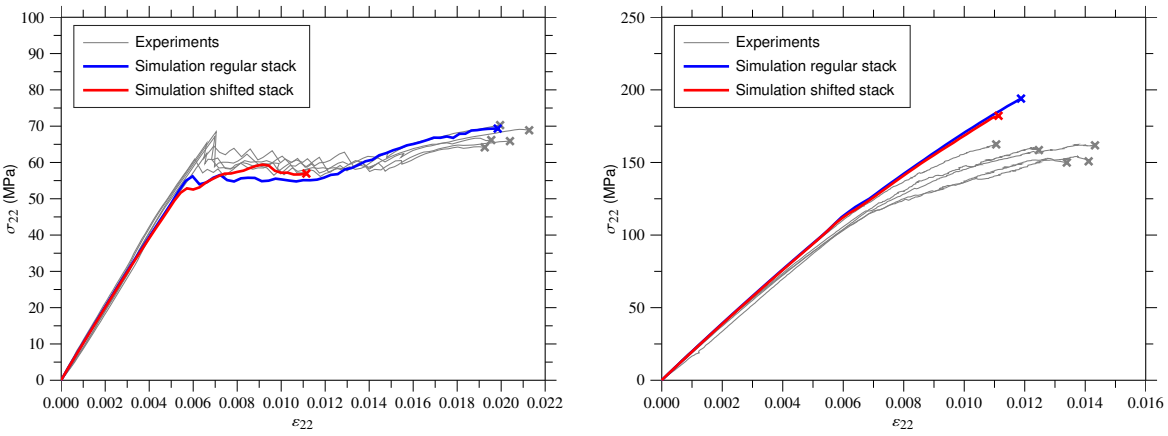

Figure 4: Stress-strain curves for loading in transverse (22) direction (a) $[0/\pm 30]$ (b) $[0/\pm 45]$

ACKNOWLEDGEMENTS

This work was funded under the UK Engineering and Physical Sciences Research Council (EPSRC) Programme Grant EP/I02946X/1 on High Performance Ductile Composite Technology in collaboration with the University of Bristol.

REFERENCES

[1] N.V. De Carvalho, S.T. Pinho, and P. Robinson. Reducing the domain in the mechanical analysis of periodic structures, with application to woven composites. *Composites Science and Technology*, 71(7):969 – 979, 2011.

[2] ST Pinho, R Darvizeh, P Robinson, C Schuecker, and PP Camanho. Material and structural response of polymer-matrix fibre-reinforced composites. *Journal of Composite Materials*, 46(19-20):2313–2341, 2012.

[3] AS Kaddour and MJ Hinton. Maturity of 3d failure criteria for fibre-reinforced composites: Comparison between theories and experiments: Part b of wwfe-ii. *Journal of Composite Materials*, 47(6-7):925–966, 2013.

Excerpt from ISBN 978-3-00-053387-7